Eur. Phys. J. A **6**, 131–140 (1999)

THE EUROPEAN PHYSICAL JOURNAL A

Lifetimes and configuration mixing in ^{110}Cd

Yu.N. Lobach[1], A.D. Efimov[2], A.A. Pasternak[2]

[1] Institute for Nuclear Research of the Ukrainian Academy of Sciences, pr. Nauki, 47, 252680 Kiev, Ukraine (e-mail: lobach@kinr.kiev.ua)
[2] Cyclotron Laboratory, A. F. Ioffe Physical Technical Institute, ul. Politechnitcheskaja, 26, 194021 St.-Petersbourg, Russia

Received: 20 March 1999 / Revised version: 28 May 1999
Communicated by D. Schwalm

Abstract. Lifetimes of excited states in ^{110}Cd have been measured by the Doppler shift attenuation method in the reaction (α,2$n\gamma$) at E_α=25 MeV. Lifetime values for 8 states and lifetime limits for 3 states were obtained. The band structures of ^{110}Cd have been interpreted in terms of a modified version of the interacting boson model (IBM + 2 q.p.). The calculations explain well the excitation energies and electromagnetic transition probabilities up to J^π=16^+, except for the 10^+_1 state. The structural features are discussed in terms of collective and two quasiparticle excitations.

PACS. 21.10.Tg Lifetimes – 21.60.Fw Models based on group theory – 23.20.Lv Gamma transitions and level energies – 27.60.+j $90 \leq A \leq 149$

1 Introduction

The previous works on ^{110}Cd [1–3] have established the detailed level scheme, in particular several 8^+ states and bands built on them have been identified. Moreover, lifetime measurements in ^{110}Cd [4,5] allow to obtain the experimental data for electromagnetic transition probabilities. At the same time the understanding of the structure of many states in this nucleus is incomplete. Largely this is due to the fact that in all experimentally observed 8^+ states, the collective component is not dominant. It means that any version of IBM which does not include two quasiparticle excitations is not suitable for the theoretical description of the states above 8^+.

In order to further investigate of the above problem we have obtained new data on the lifetimes in ^{110}Cd by the Doppler shift attenuation method using the (α,2$n\gamma$)-reaction. These data together with previously known lifetimes in this nucleus provide a good testing ground for theoretical models. The energies of excited states in ^{110}Cd and electromagnetic transition probabilities are compared with calculations within the modified version of the interacting boson model. The modification of the model is to account for phonons with multipolarities from 4 to 10 coupled to the quadrupole bosons.

2 Experimental methods and results

The experiment to measure lifetimes in ^{110}Cd was performed at the cyclotron of the A. F. Ioffe Physico-Technical Institute, St.-Petersbourg. The excited states of ^{110}Cd were populated via the reaction ^{108}Pd($\alpha, 2n\gamma$) at an incident energy of 25 MeV. The initial recoil velocity of 0.56% of the velocity of light was determined from the reaction kinematics. A self-supported enriched ^{108}Pd target of thickness 3.9 mg/cm^2 was used. The single spectra were measured with a high purity germanium detector of 30% relative efficiency and 2.2 keV energy resolution at E_γ=1.3 MeV. The detector was positioned at the angles θ = 35°, 55°, 90°, and 145° with respect to the incident beam at a distance of 16 cm from the target. Fig. 1 shows the spectrum measured at 90°, spectra with similar statistics were obtained at the other angles. The spectra obtained at 35° and 145° were used for lifetime determination. The relative intensities of the γ-transitions were determined from the spectrum measured at 55°. The spectrum at 90° was used for the determination of exact peak positions of γ-ray transitions under study as well as neigbouring weak peaks.

The lifetimes of excited states were determined by applying the Doppler shift attenuation method (DSAM) to the experimental line shapes measured at different angles. The DSAM involves a comparison of the decay time of recoils with their slowing-down time in the target. In the present work such comparison was carried out by a computer code [6], which performs a least-square fit of the calculated line shape to the experimental one regarding the level lifetime as a variable parameter. The lifetime value of an investigated level was found by a best fit of one of its decaying γ-transition and this value was accepted to be the level lifetime. The procedure was the same as that described in our previous work for ^{115}Sb [7], therefore we give here only a brief description of it.

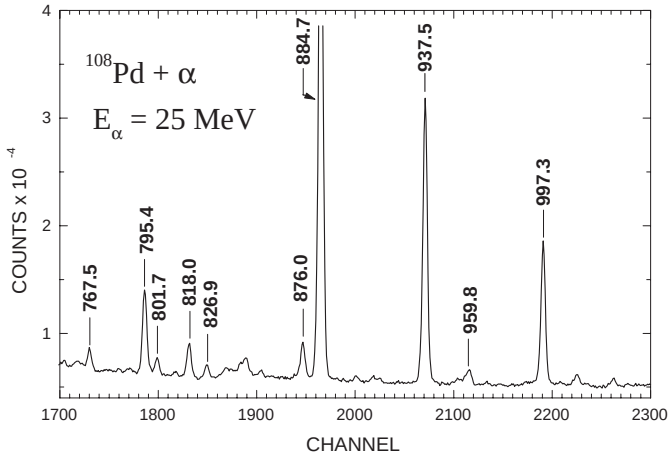

Fig. 1. γ-ray spectrum from the ^{108}Pd(α,2$n\gamma$) reaction at E_α = 25 MeV measured at 90°. Peaks marked by their energies in keV are used for lifetime determination in the present work

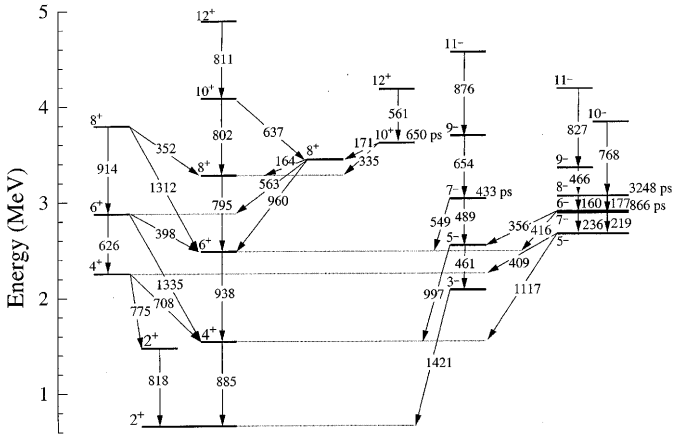

Fig. 2. Partial level scheme of ^{110}Cd (taken from [2])

The velocity and direction angles of recoils after the reaction were calculated by a code based on the statistical model of nuclear reactions. The distribution of recoils follows from the Monte Carlo simulation which takes into account reactions at different depths in the target, the kinematics of the reaction as well as the slowing-down and deflection of the recoils. About 20000 recoil histories were used in the present analysis. According to [6] the slowing-down process was assumed to have the form

$$d\varepsilon/d\rho = f_e k\varepsilon^{1/2} + f_n\varepsilon^{1/2}/(0.67\varphi_n + 2.07\varepsilon) \qquad (1)$$

where ε and ρ are the energy and range in the Lindhard's units; k is the electronic Lindhard's stopping power coefficient; f_e and f_n are the correction factors for Lindhard's cross sections for the electronic and nuclear stopping power, respectively; φ_n is an additional correction factor which characterizes the difference of the shape for the nuclear stopping power from Lindhard-Scharff-Schiott (LSS) theory [8]. The correction factors were selected as $f_e = 1.3 \pm 0.1$ and $f_n = \varphi_n = 0.9 \pm 0.1$. These values are suggested from the analysis of the slowing-down process of Cd ions in a Cd target [9].

The cascade population of the level under study was taken into account according to the decay scheme of ^{110}Cd from the (α,2nγ)-reaction given in [2] with the γ-ray transition intensities determined from the present experiment at 55° and E_α=25 MeV; the relevant level scheme considered in the present analysis is shown in Fig. 2. Thus, in the case of the 3282, 4173 and 4559 keV states, only direct feeding was considered. For the 2079 and 2540 keV states a long lifetime feeding from the 8^- at 3056 keV and 7^- at 3029 keV states was included, respectively. It was also assumed that the 4888 keV state has the effective lifetime value greater than 2 ps due to its τ=2.0±0.2 ps from [4], therefore, this effective lifetime was used for the feeding of the 4077 kev state. Finally, it was determined that the feeding from the 3791, 2877 and 2251 keV states having an unknown lifetimes to the 1476, 1542, 2480 and 2251 keV states have a small intensities which does not exceed 4% of the own population of the investigated states. It turned out from the analysis of these three states that the influence of the feeder lifetime uncertainty on the measured lifetime values is practically negligible. The side-feeding time was assumed to depend on the level energy and the position of the calculated entry region. The center of the entry region has been established to be about 3 MeV higher relative to the highest state excited in the $(\alpha, 2n\gamma)$-reaction at E_α=25 MeV. An increase of side-feeding time with a decrease of the level energy of 0.03 ps/MeV was assumed, therefore the side-feeding time for each level was kept constant and was in the range 0.09–0.18 ps. As far as the measured lifetime values are about 1 ps and more, the influence of side-feeding time and its uncertainty on the final lifetime values was rather small (< 10%) and was included in the error analysis of the measured lifetimes.

As an illustration of the DSAM the line shape analysis of some γ-transitions are shown in Figs. 3 and 4. In the analysis, the χ^2 criterion was determined by varying the τ value separately for each angle. Then the χ^2 values were averaged and normalized to unity, giving the adopted χ^2 value for both angles. The statistical error of the lifetime was determined from the value of $\chi^2_{min} + \Delta\chi^2$, where $\Delta\chi^2 = \chi^2_{min}/(nN - k)$, n is the number of angles used for lifetime determination, N is the number of channels in the peak, k is the number of varying parameters in the analysis ($k = 2-5$). Figure 3 presents a case when the lifetime value was obtained from both forward and backward angles because γ818.0 has no interfering neighbouring γ-peaks. Another case is shown in Fig. 4 for three γ-peaks when the reliable χ^2-curve must be obtained from one angle only. The lifetime values obtained from the present experiment as well as from other works [1,4,5] are given in Table 1. The lifetime errors include the statistical error, the uncertainties of the feeding and transition intensities as well as the uncertainty of nuclear and electronic stopping powers. One can see from Table 1 that our results are in agreement with the previous ones from Coulomb excitation [1] and the recoil-distance method [4] and this is evidence for the reliability of the method used.

Table 1. Experimental lifetimes of excited states in ^{110}Cd

$E_{\rm lev}$,	J^π	E_γ,	τ, (ps)			
[keV]		[keV]	[1]	[4]	[5]	present
658	2^+		7.78±0.10	9.2±0.6		
1476	2^+	818.0	0.98±0.14			1.07±0.27
1542	4^+	884.7	1.05±0.13	< 3.0		$1.18^{+0.32}_{-0.18}$
1784	2^+		$1.44^{+2.00}_{-0.60}$			
2079	3^-	1420.3				$1.05^{+0.50}_{-0.35}$
2480	6^+	937.5		< 3.0		$0.58^{+0.22}_{-0.13}$
2540	5^-	997.3				$0.90^{+0.40}_{-0.25}$
2879	7^-			1000±60[a)]	866±144	
3029	7^-				433±144	
3056	8^-			3500±500[b)]	3248±144	
3187	8^+			80±9		
3275	8^+	795.4		< 4.0		> 1.2
3346	9^-			71±4		
3428	8^-			8.6±0.8		
3440	8^+	959.8		< 4.0		> 1.6
3611	10^+			800±40[c)]	650±144	
3823	10^-	767.5		5.0±0.4		> 3.0
4077	10^+	801.7		1.0±0.3		$1.2^{+0.5}_{-0.3}$
4172	12^+			12.0±0.6		
4173	11^-	826.9		3.0±0.2		$2.5^{+2.0}_{-1.0}$
4182	10^-			1.5±0.2		
4559	11^-	876.0				$2.5^{+2.0}_{-1.0}$
4888	12^+			2.0±0.2		
5026	14^+			2.0±0.2		
5092	12^-			4.7±0.5		
5249	13^-			< 2.0		
6100	16^+			< 1.5		

E_γ - γ-ray transition used for lifetime determination in the present work.
a) $\tau = 750 \pm 40$ ps [10].
b) Taken from [3].
c) $\tau = 670 \pm 35$ ps [10].

On the basis of all known lifetimes in ^{110}Cd from Table 1 the reduced electromagnetic transition probabilities $B(\sigma{\rm L})$ were calculated and are presented in Table 2. For the states at 2879, 3056 and 3611 keV we used the lifetime values from [5] assuming them as more reliable. For the states at 3275 and 3440 keV we used the lifetime limits from the present work and [4].

3 Discussion

3.1 IBM1 description of the ^{110}Cd nucleus

The properties of positive parity states in ^{110}Cd were analyzed within the framework of a modified version of the interacting boson model [11]. This version of the model was introduced in [12,13] for the description of aligned bands in the even-mass Ru isotopes and some bands in ^{76,78}Se, ^{126,132}Ba and ^{130}Ce. Also in the framework of this model the excited states of ^{118}Te were investigated [14]. The main difference of the present calculations from previous ones is an account of real phonon states with different spins instead of fixed two-quasiparticle pairs. The structure of these states was determined in the framework of the Random Phase Approximation using factorized multipole forces. The model space includes the following boson states $\Psi^I_\Omega(d,s)$ and $(b^+_{\alpha J}\Psi^{I'}_{\Omega-1}(d,s))^I_\tau$, where I is the total angular momentum, $\Psi^I_\Omega(d,s)$ or $\Psi^{I'}_{\Omega-1}$ are d-, s-boson functions with the spin I or I' and the boson number Ω or Ω-1, respectively. The index τ denote that the collective states are formed with the presence of low collectivized phonon $b_{\alpha J}$ with predominant neutron (τ=ν) or proton (τ=π) component. The boson structure of Ψ^I_Ω and $\Psi^{I'}_{\Omega-1}$ is determined by the IBM1 Hamiltonian

$$H_{\rm IBM1} = \varepsilon_d \hat{n}_d + k_1(d^+d^+ss + h.c.) + \\ + k_2([d^+d^+]^{(2)}ds + h.c.) \\ + 1/2\sum_L C_L[d^+d^+]^{(L)}[dd]^{(L)} \qquad (2)$$

The Hamiltonian parameters were selected phenomenologically from the collective states which are well described by IBM1 (Table 3). It is well known from the experience of the IBM1 calculations that the parameter

Table 2. Reduced transition probabilities in ^{110}Cd

$E_{\rm lev}$, [keV]	τ, [ps]	J_i^π	J_f^π	E_γ, [keV]	I_γ, [%]	σL	δ[a]	$B(E2)$, [W.u.]	$B(M1)$ [10^{-3} W.u.]	$B(E1)$ [10^{-6} W.u.]
658	9.2±0.6	2_1^+	0_1^+	657.8	100	$E2$		23.0±1.5	-	-
1476	1.07±0.27	2_2^+	2_1^+	818.0	100.0(7)	$M1+E2$	-1.36(7)	29.8±7.7	13.2±3.5	-
			0_1^+	1475.8	54.3(5)	$E2$		1.3±0.3	-	-
1542	$1.18^{+0.32}_{-0.18}$	4_1^+	2_1^+	884.7	100	$E2$		40.0±8.0	-	-
1784	$1.44^{+2.00}_{-0.60}$	2_3^+	2_1^+	1125.7	100(3)	$M1+E2$	+0.33(8)	$0.77^{+0.60}_{-0.54}$	$10.4^{+7.4}_{-6.0}$	-
			0_1^+	1783.5	34(1)	$E2$		0.27±0.16	-	-
2079	$1.05^{+0.50}_{-0.35}$	3_1^-	2_3^+	295.4	3.8(2)	$(E1)$		-	-	540±200
			2_2^+	603.1	15.3(10)	$(E1)$		-	-	260±100
			2_1^+	1420.3	100(2)	$E1$		-	-	135±55
2480	$0.58^{+0.22}_{-0.13}$	6_1^+	4_3^+	229.4	0.035(3)	$E2$		24.9±7.4	-	-
			4_1^+	937.5	100.0(3)	$E2$		62.3±17.5	-	-
2540	$0.90^{+0.40}_{-0.25}$	5_1^-	3_1^-	460.9	1.7(9)	$E2$		36±22	-	-
			4_1^+	997.3	100(1)	$E1$		-	-	480±160
2879	866±144	7_1^-	5_2^-	219.3	1.9(1)	$(E2)$		0.9±0.2	-	-
			5_1^-	339.2	32.2(3)	$E2$		1.6±0.3	-	-
			6_1^+	399.3	100(1)	$E1$		-	-	5.8±1.0
3029	433±144	7_2^-	7_1^-	149.9	15.7(10)	$M1$		-	1.6±0.7	-
			5_2^-	369.2	14.4(16)	$E2$		0.6±0.3	-	-
			5_1^-	489.4	75.1(7)	$E2$		0.8±0.3	-	-
			6_1^+	549.1	100(2)	$E1$		-	-	2.9±1.0
3056	3248±144	8_1^-	6_1^-	159.7	42.2(7)	$E2$		22±1	-	-
			7_1^-	176.5	100(1)	$M1+E2$	-1.03(54)	14±7	0.51±0.26	-
3187	80±9	8_1^+	6_1^+	707.4	100	$E2$		1.9±0.2	-	-
3275[b]	1.2<...<4.0	8_2^+	6_2^+	399	1.0(2)	$E2$		13.8±6.4	-	-
			6_1^+	795.4	100(1)	$E2$		44.0±23.8	-	-
3346	71±4	9_1^-	8_1^-	290.1	10.4(2)	$M1+E2$	+0.54(19)	3.9±2.0	1.35±0.23	-
			7_1^-	466.0	100(1)	$E2$		15.1±0.9	-	-
3428[b]	8.6±0.8	8_2^-	8_1^-	371.6	14.1(12)	$M1+E2$	-0.25(15)	$3.1^{+4.1}_{-2.6}$	8.3±0.8	-
			6_1^-	531	3.5(12)	$E2$		2.4±0.8	-	-
			7_1^-	548.2	100(2)	$M1+E2$	-0.14(4)	1.3±0.3	18.8±1.9	-
3440	1.6<...<4.0	8_3^+	8_2^+	164.3	11.5(3)	$M1+E2$	-0.22(27)	<2000	245±105	-
			6_2^+	562.9	30.7(7)	$E2$		43.5±18.6	-	-
			6_1^+	959.8	100(1)	$E2$		9.8±4.2	-	-
3611[b]	650±144	10_1^+	8_3^+	171.3	15.2(4)	$E2$		33.5±8.5	-	-
			9_1^-	265.2	5.5(4)	$E1$		-	-	1.3±0.3
			8_2^+	335.6	100(1)	$E2$		7.7±1.8	-	-
			8_1^+	423.5	2.3(3)	$E2$		0.054±0.018	-	-
3823	5.0±0.4	10_1^-	9_1^-	477.5	20.0(6)	$M1+E2$	-0.24(8)	2.1±1.2	9.2±0.3	-
			8_1^-	767.5	100(1)	$E2$		16.4±1.3	-	-
4077[b]	$1.2^{+0.5}_{-0.3}$	10_2^+	8_3^+	637.2	7.5(11)	$E2$		14.8±5.1	-	-
			8_2^+	802.1	100(2)	$E2$		60.4±18.6	-	-
			8_1^+	890	<2.2	$E2$		<0.5	-	-
4172	12.0±0.6	12_1^+	10_1^+	561.0	100	$E2$		39.0±2.0	-	-
4173	3.0±0.2	11_1^-	9_1^-	826.9	100	$E2$		22.5±1.5	-	-
4182[b]	1.5±0.2	10_2^-	9_2^-	499.1	16.9(15)	$(M1+E2)$[c]		(62.2±11.2)	(19.1±3.4)	-
			8_2^-	754.9	100(6)	$E2$		46.2±7.6	-	-
			9_1^-	836.5	36.9(46)	$M1+E2$	-0.27(8)	0.74±0.41	8.3±1.7	-
			8_1^-	1026	<3	$E2$		<0.3	-	-
4559	$2.5^{+2.0}_{-1.0}$	11_2^-	10_1^-	736.7	17.4(14)	$M1+E2$	-0.07(5)	0.06±0.06	5.3±2.7	-
			9_2^-	876.0	100(2)	$E2$		19.1±9.6	-	-
4888[b]	2.0±0.2	12_2^+	10_2^+	811.1	100	$E2$		37.4±3.8	-	-
			10_1^+	1277.2	<1	$E2$		<0.04	-	-
5026	2.0±0.2	14_1^+	12_1^+	854.3	100	$E2$		28.8±2.9	-	-
5092	4.7±0.5	12_1^-	10_1^-	910.6	100	$E2$		8.9±1.0	-	-
5249	<2.0	13_1^-	11_1^-	1076.1	100	$E2$		>9.0	-	-
6100	<1.5	16_1^+	14_1^+	1074.6	100	$E2$		>12.0	-	-

[a] From [1]. [b] Branching ratio from [4]. [c] For mixed transitions with unknown mixing ratio $B(\sigma L)$ in parenthesis as for pure $E2$ or $M1$ transition.

Table 3. IBM1 parameters (e^* - $e{\cdot}fm^2$, Ω and χ - without dimension, others - MeV)

	Ω	ε	k_1	k_2	C_o	C_2	C_4	e^*	χ
					set I				
$\mid C>$	7	0.7517	-0.0358	0.0511	0.3125	−0.110	0.133	8.52	-0.21
$\mid C_\nu>$	6	0.6398	-0.0320	0.0274	0.456	0.152	0	10.04	-0.06
$\mid C_\pi>$	6	1.3950	0	0	0	0	0	9.00	0
					set II				
$\mid C>$	7	0.6050	−0.0890	0.0147	0.11	−0.161	0.0446	7.364	0.614
$\mid C_\nu>$	6	0.6211	−0.0824	0.0153	0.1469	−0.2557	0	8.715	−0.10
$\mid C_\pi>$	6	1.3950	0	0	0	0	0	9.00	0

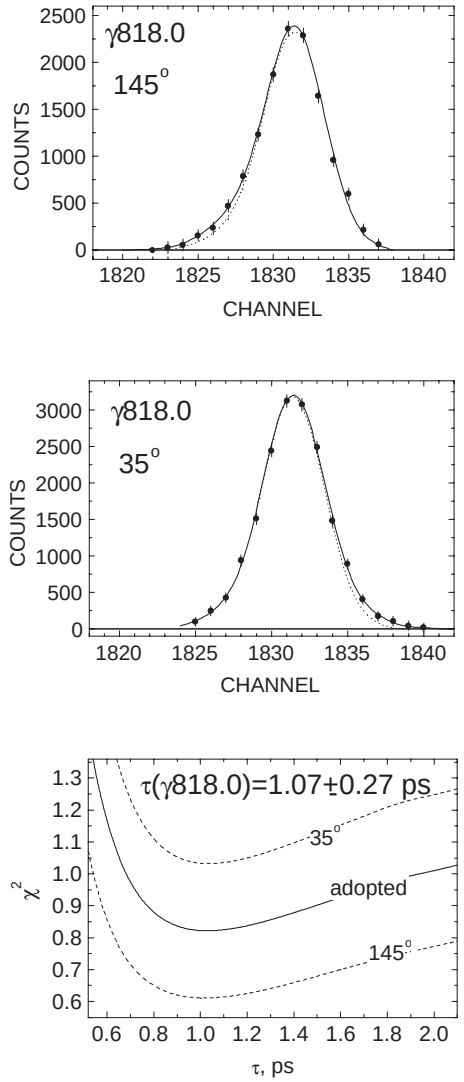

Fig. 3. Line shape analysis of background subtracted γ818.0. Solid lines are the best fit to the line shapes, the dashed lines show apparative line shapes at these experimental conditions

values depends on the energy of the 0_2^+ state. At present, it is assumed that the 0_2^+ and 2_3^+ states in ^{110}Cd belongs to the proton intruder $2p-4h$ band [4,15]. The measured $B(E2,0_2^+\to 2_1^+)$ value would be one of the verifications of such assumption. The known electromagnetic characteristic related to the 0^+ states in ^{110}Cd is only the measured ratio $B(E2,0_3^+\to 2_2^+)/B(E2,0_3^+\to 2_1^+)=171\pm 62$ [16]. Our attempts to obtain the 0_2^+ and 0_3^+ states in the calculations simultaneously among other low-lying states were unsuccessful, except the exotic cases, for example, when the 0_3^+ state is exhaused by the configuration $n_d=\vartheta=6$, where n_d is the number of quadrupole bosons, ϑ is the seniority in the $SU(5)$ basis of the IBM1. Therefore, two kinds of the calculations were performed. The low-lying 0_2^+ state was obtained in the first one. In this case the parameter fitting gave the wave functions of the collective states close $SU(5)$-limit of the IBM1. This parameter set is denoted as the set 1 in Table 3. In the second case the experimentally observed 0_3^+ state was described as the first collective state and the wave functions were turned out close to the $O(6)$-limit with the determined parameter set (denoted as the set 2 in Table 3). The overlap integrals between the eigenfunctions of the $H_{\rm IBM1}$ and $O(6)$ Hamiltonian (but not their squares) were 0.91, 0.96, 0.95, 0.97 and 0.97 for the 0_1^+, 0_2^+, 2_1^+, 4_1^+ and 6_1^+ states, respectively, in the second case. Moreover, it is interesting to note that in this case it was possible to get the ratio $B(E2,0_3^+\to 2_2^+)/B(E2,0_3^+\to 2_1^+)$ about 300. Thus, we treated the experimentaly observed 0_2^+ and 0_3^+ states as the collective quadrupole and intruder states, respectively, in the first case of the calculations, while in the second case their treatment was opposite, i.e. the 0_2^+ state was the intruder one and the 0_3^+ state was the collective one.

The symbols D and B_J stand for quasiparticle phonons, while d and b_J denote their boson counterparts. The microscopic structure of D and B_J phonons

$$D_\mu^+(B_{J\mu}^+)=1/\sqrt{2}\sum_{12}(\psi_{12}(\psi_{12}^B)(a_1^+a_2^+) + \varphi_{12}(\varphi_{12}^B)(a_{\bar 2}a_{\bar 1}))_\mu^{(J)} \quad (3)$$

was calculated using the factorized multipole-multipole isoscalar forces in the particle-hole (ph) channel. The monopole and quadrupole pairing were accounted for also in the particle-particle (pp) channel. The pairing gaps were taken from the pairing energies. The strength parameters of ph and pp quadrupole interactions were chosen so as to reproduce the parameters ε_d and k_1 in the Hamiltonian (2) [17]. Their values in the units of Bohr and Mottelson [18] were found as $k_{ph}^{(2^+)}=1.042k_{BM}^{(2^+)}$,

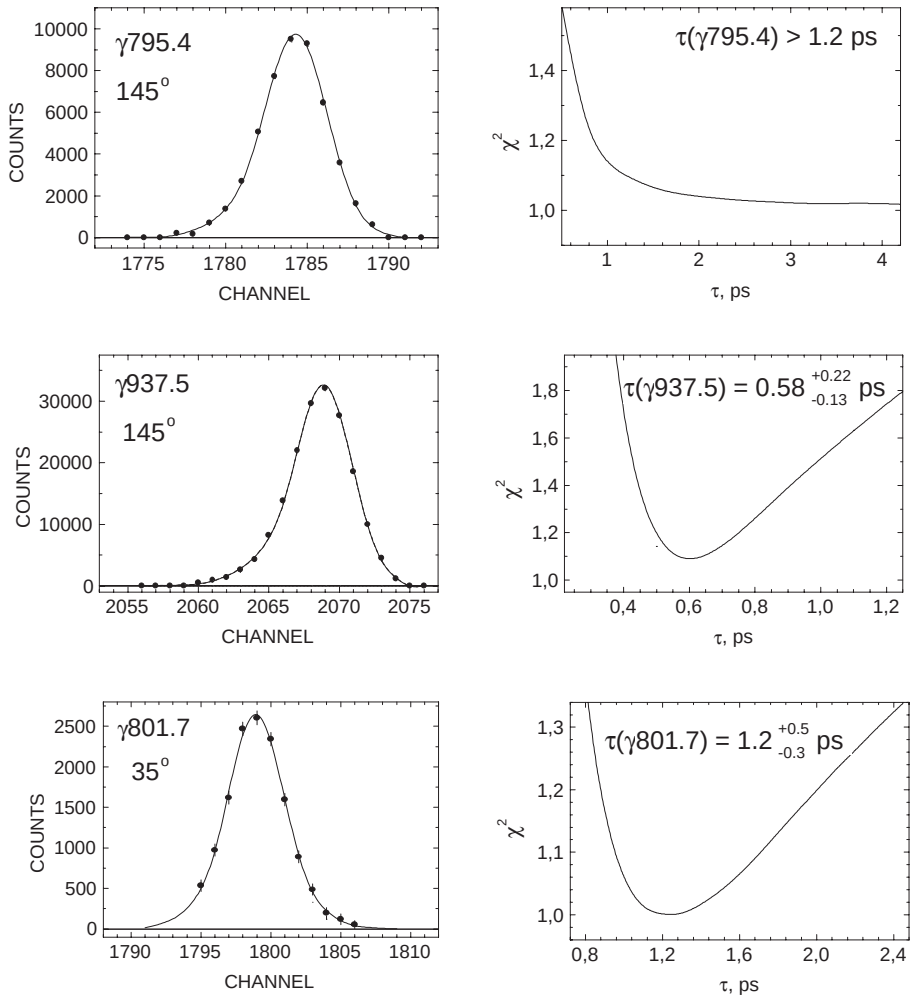

Fig. 4. The same as in Fig. 3, but for γ795.4, γ937.5 and γ801.7

$G^{(2^+)}_{\pi\pi} = G^{(2^+)}_{\nu\nu} = 1.5k^{(2^+)}_{BM}$, $G^{(2^+)}_{\pi\nu} = 0$. The parameters for higher multipolarities were taken as $k^{(4^+)}_{ph} = 0.957k^{(4^+)}_{BM}$, $k^{(6^+)}_{ph} = 0.784k^{(6^+)}_{BM}$, $k^{(8^+)}_{ph} = 0.55k^{(8^+)}_{BM}$, $k^{(10^+)}_{ph} = 0.3k^{(10^+)}_{BM}$.

The single-particle spectra were obtained with the Saxon-Woods potential. The single-particle energies were taken from [19]. Their values for the valence neutron shells $2d_{5/2}$, $1g_{7/2}$, $1h_{11/2}$, $3s_{1/2}$, $2d_{3/2}$ were 0, 1.12, 2.92, 3.62, 4.10 MeV and for the valence proton shells $1f_{5/2}$, $2p_{3/2}$, $2p_{1/2}$, $1g_{9/2}$ 0, 0.11, 2.29, 3.19 MeV, respectively. The energies of phonon states and their main components are presented in Table 4.

As described in [11–13] the interaction between $b^+_{\alpha J}\Psi^{I'}_{\Omega-1}(d,s)$ and $\Psi^I_\Omega(d,s)$, as well as between $b^+_{\alpha 1 J1}\Psi^I_{\Omega-1}(d,s)$ and $b^+_{\alpha 2 J2}\Psi^{I'}_{\Omega-1}(d,s)$ has a form

$$
\begin{aligned}
V_{\rm int} = \sum_{\alpha J}\Big[& p_{\alpha J} b^+_{\alpha J} s^+ (dd)^{(J)} \\
& + \sum_{\alpha' J'} p_{\alpha J \alpha' J'} (b^+_{\alpha J} d^+)^{(J')} (b_{\alpha' J' } s)^{(J')} + \\
& + q_{\alpha J} b^+_{\alpha J} s^+ s^+ (ddd)^{(J)} \\
& + \sum_y r^y_{\alpha J} (b^+_{\alpha J} d^+)^{(y)} (dd)^{(y)} + \\
& + \sum_{\alpha' J' y} s^y_{\alpha J \alpha' J'} (b^+_{\alpha J} (d^+ d^+)^{(y)})^{(J')} (b_{\alpha' J'} ss)^{(J')} \Big] \\
& + h.c. \; . \qquad (4)
\end{aligned}
$$

The parameter values were determined with the same multipole forces as for the phonon state structure (3).

The $B(E2)$ values were calculated with the parameters e^* and χ (Table 3) by means of

$$T_{\rm IBM1}(E2) = e^*(d^+ s + s^+ d + \chi d^+ d)^{(2)} \qquad (5)$$

The operator for $M1$-transition probabilities and gyromagnetic ratios has the form

$$T_{\rm IBM1}(M1) = \sqrt{10} g_d (d^+ d)^{(1)} + \sum_\lambda g_\lambda (b^+_\lambda b_\lambda)^{(1)} \qquad (6)$$

where g_d and g_λ were calculated including the phonon amplitudes (3) and the spin gyromagnetic ratio equal to 0.6 of the free nucleon value.

Table 4. Energies and main amplitudes ψ wave function of the phonons used in calculations

J^π	E [MeV]	$\nu d^2_{5/2}$	$\nu g_{7/2}d_{5/2}$	$\nu g^2_{7/2}$	$\nu h^2_{11/2}$	$\nu s_{1/2}d_{5/2}$	$\nu s_{1/2}g_{7/2}$	$\nu d_{3/2}g_{7/2}$	$\pi g^2_{9/2}$
2^+_1	0.707	0.23	0.10	0.53	-0.42	-0.19	-	-0.22	0.42
4^+_1	2.106	-0.15	-0.21	-0.60	0.29	-	-0.21	0.15	-0.45
6^+_1	2.675	-	0.30	0.78	-0.16	-	-	-	0.40
8^+_1	2.990	-	-	-	-	-	-	-	1.00
8^+_2	3.925	-	-	-	1.00	-	-	-	-
10^+_1	3.971	-	-	-	1.00	-	-	-	-

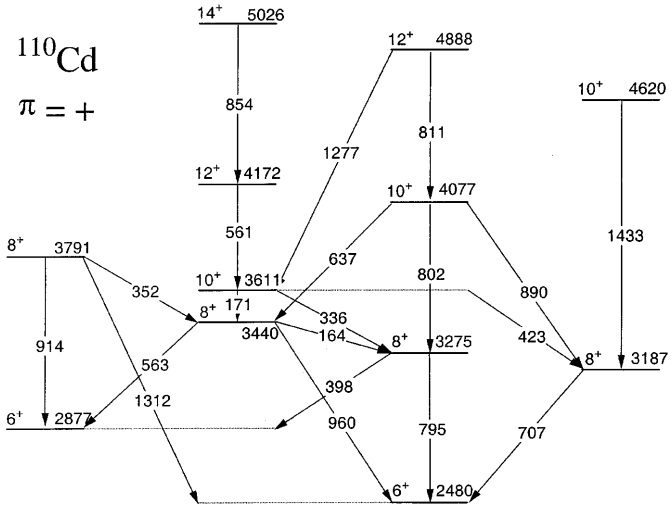

Fig. 5. Partial level scheme of positive parity states in ^{110}Cd (taken from [2,3])

Table 5. Experimental and calculated $B(E2)$ in ^{110}Cd

J^π_i	J^π_f	E_γ,	$B(E2)$ [W.u.]		
		[keV]	exp.	calc.I	calc.II
2^+_1	0^+_1	658	23.0±1.5	23	23
0^+_2	2^+_1			21	
2^+_2	0^+_1	1476	1.3±0.2	1.4	1.0
2^+_2	2^+_1	818	30±8	23	33
4^+_1	2^+_1	885	40.0±8.0	35	31
6^+_1	4^+_1	938	62.3±17.5	38	32
8^+_1	6^+_1	707	1.9±0.2	0.6	3.2
8^+_2	6^+_1	795	44.0±23.8	27	24
	6^+_2	399	13.8±6.4	4	2.1
8^+_3	6^+_1	960	9.8±4.2	5.0	5.4
	6^+_2	563	43.5±18.6	16	17
	8^+_2	164	$B(M1)$=0.245±0.105 W.u.	0.190	0.284
10^+_1	8^+_1	424	0.054±0.018	0.054	0.067
	8^+_2	336	7.7±1.8	0.5	0.4
	8^+_3	171	33.5±8.5	0.5	1.0
10^+_2	8^+_1	890	< 0.5	5.8	7.1
	8^+_2	802	< 35.7	19	22
	8^+_3	637	< 8.4	11.4	2
12^+_1	10^+_1	561	39.0±2.0	26	23
12^+_2	10^+_1	1277	< 0.04	0.002	0
	10^+_2	811	37.4±3.8	38	27
14^+_1	12^+_1	854	28.8±2.9	40	35
16^+_1	14^+_1	1075	> 12.0	42	34

3.2 Comparison with calculations

Two kinds of the calculations were performed in accordance with the two sets of the parameters given in Table 3. The partial level scheme of positive parity states in ^{110}Cd relevant to the present calculations is shown in Fig. 5. In Fig. 6, the comparison of the experimental and calculated excitation energies is given. The calculated transition probabilities are presented in Table 5 and denoted as calc.I and calc.II, respectively. The main components of wave functions of the states under study are presented in Table 6.

One can see a good description of the excitation energies in the framework of model used. At the same time, using of the set 1 in the calculations gave a better description in comparison with the set 2. In the case of the set 1, the difference between the calculated and experimental excitation energies does not exceed 100 keV, except for the 14^+_2 and 16^+_2 states.

The calculated $B(E2)$ values are in agreement with the experimental ones for a great number of transitions for both parameter sets. The main difference between the two kinds of calculations is connected with the $10^+_2 \to 8^+_3$ transition. In the second case, the $B(E2, 10^+_2 \to 8^+_3)$ value is significantly lower than in the first case because the wave function of the 10^+_2 state has a greater pure collective component in the second case (see Table 6). Moreover, this componet has the opposite phase relativelly the main component $(6^q_1 4_1)$ of the 10^+_2 state in contrast to the 8^+_3 state where these components have the same phases.

A dramatic divergence exists between the calculated and experimental $B(E2)$ values for the $10^+_1 \to 8^+_2$ and $10^+_1 \to 8^+_3$ transitions. A large experimental $B(E2, 10^+_1 \to 8^+_3) = 33.5\pm8.5$ W.u. must be a hint that both 10^+_1 and 8^+_3 states have a close quasiparticle structures and the main difference is due to the quadrupole d boson. However, this treatment is in contradiction with the low γ-transition energy between them. An attempt to improve the description of $B(E2, 10^+_1 \to 8^+_3)$ was done in the framework of the model by varying the parameters of multipole forces $k^{(\lambda)}_{ph}$ and parameters of the IBM1 Hamiltonian so that the main component of the 10^+_1 state wave function does not include the two quasiparticle configuration $\nu(h^2_{11/2})^{(10^+)}$. As a result $B(E2) \simeq 10$ W.u. was obtained, but at the same time the $B(E2)$ values from 8^+_i states are no more reproduced. Another possibility to explain the $B(E2, 10^+_1 \to 8^+_3)$ value could be an assignment of the configuration $(10^+_q 2_1)$ to

Table 6. Wave functions for ^{110}Cd. (I_i) means a purely collective d, s boson state with a spin I_i, $(J_i^q I_j)$ corresponds to a configuration with a b_J boson under a collective state with spin I_j. Absolute values of amplitudes presented are more than 0.1

State	Main components of wave function				
			set I		
2_1^+	$1.00(2_1)$				
0_2^+	$0.97(0_2)$	$+\,0.22(4_1^q4_1)$			
2_2^+	$0.97(2_2)$	$+\,0.18(4_1^q2_1)$			
4_1^+	$0.97(4_1)$	$+\,0.16(4_1^q0_1)$			
4_2^+	$-0.15(4_1)$	$+0.14(4_2)$	$+\,0.88(4_1^q0_1)$	$-0.36(4_1^q2_1)$	$-0.15(4_1^q2_2)$
6_1^+	$+0.90(6_1)$	$+0.33(4_1^q2_1)$	$-0.17(6_1^q0_1)$	$-0.12(6_1^q2_2)$	
6_2^+	$0.18(6_1)$	$+\,0.18(4_1^q2_2)$	$+\,0.28(4_1^q4_1)$	$+\,0.86(6_1^q0_1)$	$+\,0.31(6_1^q2_1)$
8_1^+	–	$-0.28(6_1^q2_1)$	$+0.87(8_1^q0_1)$	$+0.35(8_1^q2_1)$	
8_2^+	$0.56(8_1)$	$+\,0.57(4_1^q4_1)$	$-0.46(6_1^q2_1)$	$-0.20(8_1^q0_1)$	
8_3^+	$0.35(8_1)$	$0.41(4_1^q4_1)$	$0.21(4_1^q6_1)$	$0.68(6_1^q2_1)$	$0.23(6_1^q4_1)$
		$0.21(8_1^q0_1)$	$0.16(8_2^q0_1)$		
8_4^+		$-0.14(4_1^q6_1)$	$-0.15(6_1^q2_1)$	$-0.17(6_1^q4_1)$	$0.70(8_2^q0_1)$
		$-0.36(8_2^q2_1)$	$0.47(10_1^q2_1)$	$-0.18(10_1^q2_2)$	$-0.13(10_1^q4_1)$
10_1^+	–	$+\,0.22(8_2^q2_1)$	$+\,0.74(10_1^q0_1)$	$-0.58(10_1^q2_1)$	$-0.13(10_1^q2_2)$
		$+\,0.20(10_1^q4_1)$			
10_2^+	$-0.14(10_1)$	$-0.25(4_1^q6_1)$	$+\,0.16(4_1^q6_2)$	$+\,0.25(4_1^q8_1)$	$+\,0.82(6_1^q4_1)$
		$+0.12(6_1^q4_2)$	$+0.16(6_1^q6_1)$	$-0.13(8_1^q2_1)$	$+0.25(8_2^q2_1)$
10_3^+	$0.47(10_1)$	$0.40(4_1^q8_1)$	$-0.14(4_1^q10_1)$	$-0.24(4_2^q6_1)$	$+\,0.21(6_1^q6_1)$
		$+\,0.64(8_1^q2_1)$	$+\,0.13(8_1^q2_2)$	$0.17(8_1^q4_1)$	
12_1^+	–	$+\,0.29(8_2^q4_1)$	$+\,0.81(10_1^q2_1)$	$-0.25(10_1^q2_2)$	$-0.41(10_1^q4_1)$
		$+\,0.14(10_1^q6_1)$			
12_2^+	–	$+\,0.13(4_1^q8_2)$	$+\,0.23(4_1^q10_1)$	$+\,0.89(6_1^q6_1)$	$+\,0.17(6_1^q8_1)$
		$+\,0.24(8_2^q4_1)$			
14_1^+	–	$+\,0.31(8_2^q6_1)$	$+\,0.84(10_1^q4_1)$	$-0.25(10_1^q4_2)$	$-0.35(10_1^q6_1)$
14_2^+	–	$+0.41(4_1^q10_1)$	$+0.87(6_1^q8_1)$	$+0.13(6_1^q10_1)$	$+0.20(8_2^q6_1)$
16_1^+	–	$+0.32(8_2^q8_1)$	$+0.86(10_1^q6_1)$	$-0.22(10_1^q6_2)$	$-0.31(10_1^q8_1)$
			set II		
2_1^+	$1.00(2_1)$				
0_3^+	$0.94(0_2)$	$+\,0.34(4_1^q4_1)$			
2_2^+	$0.97(2_2)$	$+\,0.20(4_1^q2_1)$			
4_1^+	$0.97(4_1)$	$+\,0.14(4_1^q0_1)$	$-0.14(6_1^q2_1)$		
4_2^+	$-0.11(4_1)$	$0.59(4_2)$	$+\,0.74(4_1^q0_1)$	$-0.25(4_1^q2_1)$	
6_1^+	$0.89(6_1)$	$+0.23(4_1^q2_1)$	$-0.31(6_1^q0_1)$	$-0.19(6_1^q2_2)$	
6_2^+	$+0.23(6_1)$	$+0.14(4_1^q2_1)$	$+0.20(4_1^q2_2)$	$+0.19(4_1^q4_1)$	$+0.84(6_1^q0_1)$
		$+0.35(6_1^q2_1)$			
8_1^+	$0.19(8_1)$	$-0.31(6_1^q2_1)$	$0.85(8_1^q0_1)$	$0.34(8_1^q2_1)$	
8_2^+	$0.63(8_1)$	$+\,0.23(4_1^q4_1)$	$-0.58(6_1^q2_1)$	$-0.11(6_1^q2_2)$	$-0.14(6_1^q4_2)$
		$-0.34(8_1^q0_1)$	$-0.14(8_1^q2_1)$	$-0.16(8_2^q0_1)$	
8_3^+	$0.54(8_1)$	$0.31(4_1^q4_1)$	$0.23(4_1^q4_2)$	$0.20(4_1^q6_1)$	$0.54(6_1^q2_1)$
		$0.24(6_1^q4_1)$	$-0.10(6_1^q4_2)$	$+\,0.26(8_2^q0_1)$	$+\,0.13(10_1^q2_1)$
8_4^+	$-0.13(8_1)$	$+0.24(8_2)$	$+0.17(4_1^q4_1)$	$-0.12(4_1^q6_1)$	$-0.22(6_1^q2_1)$
		$-0.25(6_1^q2_2)$	$-0.17(6_1^q4_1)$	$+0.58(8_2^q0_1)$	$-0.33(8_2^q2_1)$
		$+0.45(10_1^q2_1)$	$-0.19(10_1^q2_2)$	$-0.12(10_1^q4_1)$	
10_1^+		$+0.21(8_2^q2_1)$	$+0.74(10_1^q0_1)$	$-0.58(10_1^q2_1)$	$-0.17(10_1^q2_2)$
		$+0.19(10_1^q4_1)$			
10_2^+	$-0.48(10_1)$	$-0.14(4_1^q6_1)$	$+\,0.76(6_1^q4_1)$	$+\,0.15(6_1^q4_2)$	$-0.12(8_1^q2_1)$
		$+0.30(8_2^q2_1)$	$+0.13(10_1^q2_2)$		
10_3^+		$0.53(4_1^q6_1)$	$+0.28(6_1^q4_1)$	$+0.16(6_1^q6_1)$	$-0.18(6_2^q4_1)$
		$+\,0.69(8_1^q2_1)$	$+\,0.16(8_1^q2_2)$	$+\,0.20(8_1^q4_1)$	
12_1^+	–	$+\,0.27(8_2^q4_1)$	$+\,0.82(10_1^q2_1)$	$-0.30(10_1^q2_2)$	$-0.37(10_1^q4_1)$
12_2^+	$-0.50(12_1)$	$+0.76(6_1^q6_1)$	$+0.20(6_1^q6_2)$	$+0.27(8_2^q4_1)$	
14_1^+	–	$+\,0.27(8_2^q6_1)$	$+\,0.86(10_1^q4_1)$	$-0.33(10_1^q4_2)$	$-0.29(10_1^q6_1)$
14_2^+	–	$-0.33(4_1^q10_1)$	$-0.43(6_1^q8_1)$	$+0.67(6_1^q8_2)$	$-0.42(8_2^q6_1)$
		$-0.24(10_1^q4_2)$			
16_1^+	–	$+0.24(8_2^q8_1)$	$-0.15(8_2^q8_2)$	$+0.90(10_1^q6_1)$	$-0.22(10_1^q6_2)$
		$-0.20(10_1^q8_1)$	$+0.14(10_1^q8_2)$		

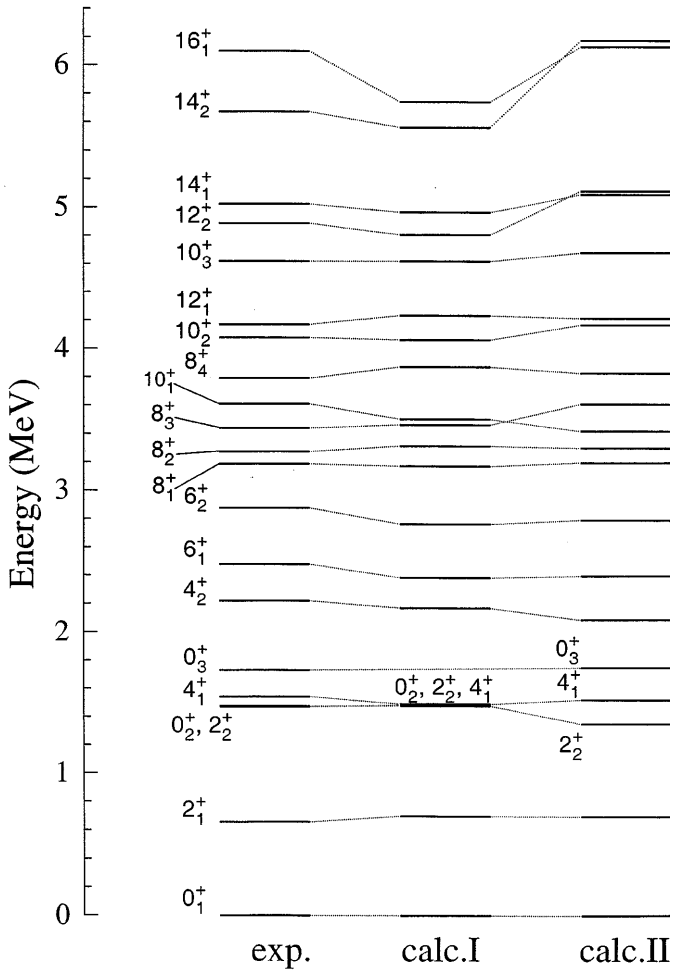

Fig. 6. Comparison of the calculated and experimentally observed excitation energies of positive parity states in ^{110}Cd

the 8_3^+ state. However, in this case $B(E2, 8_3^+ \to 6_2^+)$ value became significantly lower. Therefore, one can conclude that this model cannot explain the $B(E2, 10_1^+ \to 8_3^+)$ value in ^{110}Cd with the above assumptions. A similar experimental situation exists in the neigbouring ^{108}Cd nucleus. Although the energy of the relevant transition in ^{108}Cd is larger than in ^{110}Cd and equal to 292 keV, the $B(E2, 10_1^+ \to 8_3^+) = 25 \pm 3$ W.u. is still large [20]. A significant difference of the $B(E2)$ values exists also for the $10_2^+ \to 8_1^+$ transiton. The calculated value is at least five times bigger as the experimental one. Probably, this is caused by the increased amplitude of the $6_1^q 2_1$ component in the wave function of the 8_1^+ state which is created mainly by the quasiparticle pair $\pi(g_{9/2}^2)^{(8^+)}$.

The 8_4^+ state at 3791 keV decays by three γ-ray transitions with the relative intensity ratios $I_\gamma(8_4^+ \to 8_3^+) : I_\gamma(8_4^+ \to 6_2^+) : I_\gamma(8_4^+ \to 6_1^+) = 16 : 64 : 50$ [2]. The calculated ratios were 15:28:1.3 and 15:16:0.1 for both cases of the calculations, respectively. The small values of the last member of these ratios are due to the small calculated $B(E2, 8_4^+ \to 6_1^+)$ values equal to $8.9 \cdot 10^{-3}$ and $2.1 \cdot 10^{-3}$ W.u. in both cases, respectively. The calculated relative intensity of the $8_4^+ \to 6_1^+$ transition must be changed significantly when the wave function of the 8_4^+ state is altered. One can see from Table 6 that both kinds of the calculations gave the similar quasiparticle structure of the 8_4^+ state which is determined by the $\nu(h_{11/2}^2)^{(8^+)}$ and $\nu(h_{11/2}^2)^{(10^+)}$.

It is necessary to note a small, but a principal excess of the experimental $B(E2)$ values for the $4_1^+ \to 2_1^+$ and $6_1^+ \to 4_1^+$ transitions in comparison with the calculated ones. It is known from IBM calculations that the finite number of bosons due to cutoff factor of s bosons in the $T(E2)$-operator leads to a decreased $B(E2)$ values along the yrast-band with increasing spin in comparison with the case when a large number of bosons are used, i.e. s bosons are absent in the $T(E2)$-operator. The mentioned excess gives evidence that the calculations must be done with an increased boson number Ω or by a modified $T(E2)$-operator. For this purpose the additional calculations was performed using $T(E2) = e_1(d^+ + d + \chi_1 d^+ d)^{(2)}$, i.e. without cutoff factor. As the result, the use of such $T(E2)$-operator gives a better description of $B(E2)$ values, in particular, the $B(E2, 4_1^+ \to 2_1^+)$ and $B(E2, 6_1^+ \to 4_1^+)$ values increase on 14 and 31 %, respectively.

Looking at the components of wave functions in Table 6, one can conclude that the 2_1^+, 2_2^+, 4_1^+ and 6_1^+ states are mainly collective states as well as the 0_2^+ state in the first case and the 0_3^+ in the second one. The structures of the 4_2^+ and 6_2^+ states are mainly determined by phonon states with multipolarities 4^+ and 6^+, respectively. The main component of the 8_1^+ state is due to the proton pair $\pi(g_{9/2}^2)^{(8^+)}$ (see also Table 4). The band built on such state must be determined by quadrupole phonons which are formed under the condition of blocking of the two-quasiparticle states in the proton system. As the ^{110}Cd nucleus has 48 protons, this leads to a closed proton shell, i.e. in this case the quadrupole collectivity is formed under conditions similar to the ^{112}Sn nucleus. This peculiarity was accounted for in the calculations by an appropriate choice of the parameters for $\Psi_{\Omega-1}(d, s)_\pi$ in the Hamiltonian (see Table 3). Since $B(E2, 2_1^+ \to 0_1^+) = 15.3 \pm 0.9$ W.u in ^{112}Sn is quite large in spite of a large excitation energy of the 2_1^+ state (1257 keV), the relevant transition must be observed in ^{110}Cd. Really, such a γ-transition is observed from the 10^+ state at 4620 keV in ^{110}Cd (see Fig. 5). Among the calculated 10^+ states this state corresponds to the 10^+ one which is distinguished from other 10^+ states by a large $B(E2)$ value to the 8_1^+ state. One see from Table 6 where this 10^+ state is denoted as the 10_3^+, that the $\pi(g_{9/2}^2)^{(8^+)} \otimes 2_1^+(\pi)$ component is the most in the wave function of this state. Therefore, our treatment of the 8_1^+ and 10_3^+ states is the same as in [4] and [21], respectively.

The 8_2^+ and 8_3^+ states are formed by mixing several configurations which include both a collective component and phonons with 4^+ and 6^+. The $B(M1, 8_3^+ \to 8_2^+)$ is determined by the amplitudes of different phonons as well as the structures of the 8_3^+ and 8_2^+ states (Table 6). So far

as the calculated $B(M1, 8_3^+ \rightarrow 8_2^+)$ values in both cases agrees with the experimental one we suppose that the structures of these states are described reasonably well.

At higher spins beginning from 10^+, the component $\nu(h_{11/2}^2)^{(10^+)}$ is dominant. The calculated $g(10_1^+) = -0.16$ is not in agreement with the experimental one equal to – 0.09(3) [21]. The theoretical description of $g(10_1^+)$ must be improved by increasing the collective component in this state or the components which include 4^+ or 6^+ phonons. However, the present calculations cannot increase significantly such components in the 10_1^+ state. This fact as well as the problem of describing the $B(E2)$ values from the 10_1^+ state to the 8_3^+ and 8_2^+ ones remain an open question about the nature of the 10_1^+ state. The measured $B(E2, 10_2^+ \rightarrow 8_2^+) = 74 \pm 24$ W.u. [4] allowed to treat the 10_2^+ state at 4078 keV as the state belonging to the ground state band. Although our $B(E2)$ is smaller, it remain still large. As follows from Table 6 the structure of the 10_2^+ state is determined by the $\nu(g_{7/2}^2)^{(6^+)}$ configuration while the pure collective component is minor (about -0.14 in the first case). The calculated $B(E2, 10_2^+ \rightarrow 8_2^+)$ is in reasonable agreement with the experimental one.

Summarizing, one can note that the distinction between two kinds of our calculations is related only with the IBM1 parameters which were selected phenomenologically. These parameters were substantially different in both cases of calculations. As a result, the boson composition of the collective states turned out different too. However, the amplitudes of the wave functions are not so much different in the basis of collective and quasiparticle states and this leads to a decreased difference of the excitation energies and $B(E2)$ values for both cases of calculations. The definitive choice of the IBM1 parameter set would be facilitated by the experimentally determined $B(E2, 0_2^+ \rightarrow 2_1^+)$ value.

4 Conclusions

The lifetime values for 8 states and lifetime limits for 3 states in ^{110}Cd were obtained by DSAM with the (α,2nγ)-reaction. The structure of excited states and electromagnetic transition probabilities have been investigated in the framework of a modified version of IBM1. The comparison with calculations based on this model has helped to explain the complicated behavior and some features of nuclear structure in this nucleus. In particular, one can conclude that a reasonable description of the 2_1^+, 4_1^+, 6_1^+, 8_1^+, 8_2^+, 8_3^+, 10_2^+, 12_1^+, 14_1^+, 14_2^+ and 16_1^+ states was obtained. The structure of the 10_1^+ state is still unclear. The theoretical description of the 4_2^+ and 6_2^+ states is based on their excitation energies only because the lifetimes of these states are unknown up to now. Like this, further investigations of the electromagnetic properties in ^{110}Cd and its neighbours are of large interest.

We would like to thank R.S. Chakrawarthy for critical reading of the manuscript.

References

1. D. De Frenne, E. Jacobs, Nucl. Data Sheets **67**, 809 (1992)
2. J. Kern, A. Bruder, S. Drissi, V.A. Ionescu, Nucl. Phys. **A512**, 1 (1990)
3. S. Juutinen, R. Julin, M. Piiparinen, P. Ahonen, B. Cederwall, C. Fahlander, A. Lampinen, T. Lönnroth, A. Maj, S. Mitarai, D. Müller, P. Simecek, M. Sugawara, I. Thorslund, S. Törmänen, A. Virtanen, R. Wyss, Nucl. Phys. **A573**, 306 (1994)
4. M. Piiparinen, R. Julin, S. Juutinen, A. Virtanen, P. Ahonen, C. Fahlander, J. Hattula, A. Lampinen, T. Lönnroth, A. Maj, S. Mitarai, D. Müller, J. Nyberg, A. Pakkanen, M. Sugawara, I. Thorslund, S. Törmänen, Nucl. Phys. **A565**, 671 (1993)
5. L.K. Kostov, W. Andrejtscheff, L.G. Kostova, L. Käubler, H. Prade, R. Schwengner, Eur. Phys. J. **A2**, 269 (1998)
6. I.Kh. Lemberg, A.A. Pasternak, *Modern Methods of Nuclear Spectroscopy* (Nauka, Leningrad 1985)
7. Yu.N. Lobach, D. Bucurescu, Phys. Rev. **C57**, 2880 (1998)
8. I. Lindhard, M. Scharff, H.E. Schiott, Dan. Vidensk. Selsk. Mat. Fys. Medd. **33**, 1 (1963)
9. I.Kh. Lemberg, A.A. Pasternak, Nucl. Instrum. Methods **140**, 71 (1977)
10. M. Piiparinen, private communication
11. A.D. Efimov, V.M. Mikhajlov, Phys. Rev. **C59**, 3153 (1999)
12. A.D. Efimov, V.M. Mikhajlov, Izv. RAS, ser.fiz. **61**, 661 (1997)
13. A.D. Efimov, V.M. Mikhajlov, Izv. RAS, ser.fiz. **62**, 913 (1998)
14. A.D. Efimov, Yu.N. Lobach, Yad. Fiz. **61**, 401 (1998)
15. M. Déléze, S. Drissi, J. Kern, P.A. Tercier, J.P. Vorlet, J. Rikovska, T. Outsuka, S. Judge, A. Williams, Nucl. Phys. **A551**, 269 (1993)
16. A. Giannatiempo, A. Nannini, A. Perego, P. Sona, Phys. Rev. **C41**, 1167 (1990)
17. A.D. Efimov, V.M. Mikhajlov, *Collective nuclear dynamics* (Nauka, Leningrad 1990)
18. A. Bohr, B.R. Mottelson, *Nuclear structure*, vol.2 (Benjamin, New York 1975)
19. K. Kumar, B. Remaud, P. Aguer, J.S. Vaagen, A.C. Rester, R. Foucher, J.H. Hamilton, Phys. Rev. **C16**, 1235 (1977)
20. I. Thorslund, C. Fahlander, J. Nyberg, M. Piiparinen, R. Julin, S. Juutinen, A. Virtanen, D. Müller, H. Jensen, M. Sugawara, Nucl. Phys. **A568**, 306 (1994)
21. P.H. Regan, A.E. Stuchbery, S.S. Anderssen, Nucl. Phys. **A591**, 533 (1995)